

# Adjacent Possible Innovation Dynamics on Local Optima Networks

Leonardo Rizzo<sup>1,2</sup>, Edward D. Lee<sup>3,4</sup>, and János Kertész<sup>1</sup>

<sup>1</sup>Central European University, Department of Network and Data Science, Vienna, Austria

<sup>2</sup>SDA Bocconi, Network Innovation Lab, Milan, Italy

<sup>3</sup>Complexity Science Hub, Vienna, Austria

<sup>4</sup>University of Natural Resources and Life Sciences, Vienna, Austria

## Abstract

We propose Local Optima Networks (LONs) as a formal framework for modeling innovation dynamics. A LON is a directed weighted graph in which nodes represent locally stable technological configurations and edges encode transition probabilities between their basins of attraction. We construct LONs from fitness landscapes and model innovating agents as stochastic walkers exploring the adjacent possible on the resulting network. We show that this model simultaneously generates the four main empirical regularities of the discovery-process tradition: sublinear novelty growth (Heaps' law), heavy-tailed frequency distributions (Zipf's law), anomalous fluctuation scaling (Taylor's law), and power-law distributed inter-event times. The exponents fall within empirically observed ranges and are jointly constrained by LON topology. Communities in the LON provide an operational definition of technological paradigms grounded in basin-level accessibility. The LON framework thus bridges the discovery-process and adaptive-search traditions of innovation modeling within a single, parsimonious, and empirically testable representation.

**Keywords:** local optima networks, fitness landscapes, adjacent possible, innovation dynamics, Heaps' law, Zipf's law, Taylor's law, inter-event times, technological paradigms, path dependence

## 1 Introduction

Formal models of innovation have largely pursued two related but distinct explanatory tasks. One tradition studies the realized record of novelty as a temporally ordered sequence and asks why new types appear sublinearly, why reuse is heavy tailed, why fluctuations scale anomalously, why discoveries arrive in correlated bursts, and why inter-discovery waiting times follow heavy-tailed distributions. We refer to this as the *discovery-process* tradition; it is now much broader than a single urn-with-triggering benchmark: it encompasses species-sampling and Poisson–Dirichlet baselines, adjacent-possible urns, explicit treatments of Taylor's law, network exploration models on concept graphs, socially interacting discovery processes, and recent damped or time-dependent urn schemes designed to accommodate departures from pure power laws (Blackwell and MacQueen, 1973; Pitman and Yor, 1997; Tria et al., 2014, 2018; Iacopini et al., 2018; De Marzo et al., 2022; Aletti and Crimaldi, 2021; Bellina et al., 2025). A second tradition studies

innovation as search over a performance landscape and asks how interdependent design choices shape path dependence, local trapping, incremental improvement, and escape to qualitatively new technological approaches. We refer to this as the *adaptive-search* tradition; it is also richer than a single NK benchmark, examining decomposability, modularity, hierarchy, cognitive representations, sequencing, distributed search, competition, and ecosystem interdependence (Dosi, 1982; Kauffman, 1993; Levinthal, 1997; Baumann et al., 2019; Frenken, 2006b,a; Billinger et al., 2014; Ganco et al., 2020).

The two traditions typically operate at different levels of description. Discovery models explain sequence-level observables such as novelty growth, revisit frequencies, fluctuation scaling, and temporal clustering. Adaptive-search models explain how interdependent choice architectures and search rules shape movement through a performance space. What is still missing is a representation that connects these two levels of description in a single framework.

This paper proposes that *Local Optima Networks* (LONs) can play the bridging role between the two approaches. A LON is a directed weighted graph derived from a performance landscape, with nodes representing local optima and edges representing transition relations between their basins of attraction (Ochoa et al., 2008; Vérel et al., 2011; Ochoa et al., 2014). In the combinatorial-optimization literature, LONs have been used to characterize search difficulty and global landscape structure, but they remain largely untapped in innovation economics (Khraisha, 2020). Their appeal here is that they preserve performance information while also generating a natural state space for stochastic innovation records.

The LON representation is useful for innovation modeling for three related reasons. First, it provides a basin-level representation of technological search. In our framework, a performance landscape encodes the space of configurations and associated performance values for a given technology. The LON is a coarse-graining of that landscape: its nodes are local optima, and its edges encode transitions between their basins. Prolonged residence in the same basin or repeated returns to the same optimum correspond to incremental exploitation; transitions across basins within the same community correspond to local re-orientation within a technological approach; and transitions across community boundaries correspond to a shift from one technological paradigm to another. The LON therefore offers an operational two-level vocabulary for describing innovation dynamics: basins for incremental innovation, and communities for distinct technological approaches.

Second, the LON links landscape structure to discovery-process observables. A stochastic walk on a LON generates a time-ordered sequence of visited optima, which can be read as an innovation record. The statistical properties of that record, including novelty growth, revisit concentration, fluctuation scaling, and inter-event time distributions, depend on the topology of the LON: self-loop and residence-time structure affect exploitation intensity, local connectivity shapes the reachable frontier of new states, and community structure affects waiting times, burstiness, and temporal clustering. In Section 5, we show that suitably parameterized walks on LONs generate the main empirical signatures usually associated with discovery-process models: sublinear novelty growth (Heaps' law), heavy-tailed reuse (Zipf's law), anomalous fluctuation scaling (Taylor's law), and power-law distributed inter-event times.

Third, the LON makes structural assumptions explicit and interpretable. In the baseline

model developed below, effective ruggedness is summarized by a persistence parameter  $\rho$  and a small set of additional search parameters. We treat  $\rho$  as a reduced-form proxy for a broader family of structural properties, including ruggedness, basin persistence, and effective connectivity, rather than as a literal one-to-one substitute for the full landscape literature. This keeps the model parsimonious while still allowing us to study how changes in landscape structure reshape the induced LON and, through it, the realized innovation record.

A final conceptual clarification concerns the unit of novelty. Discovery models often move between events that are new to a focal process and events that are new to the whole system. Throughout the paper, it is useful to distinguish *local novelty* (new to the focal walk, inventor, or firm) from *system-level novelty* (new to the entire interacting population). The LON framework can accommodate both notions, but the distinction should be kept explicit.

In terms of contributions, we develop the LON-based model of innovation dynamics sketched above and show that it generates the main empirical regularities emphasized by the discovery-process literature while retaining the basin-level, performance-ordered structure emphasized by the adaptive-search literature. We characterize, numerically, how LON structure constrains macroscopic innovation outcomes, including the pace of novelty growth, the distribution of revisits across states, the emergence of bursty or heavy-tailed inter-event times, and the fluctuation scaling of innovation counts.

The remainder of the paper is organized as follows. Section 2 reviews the two modeling traditions in a way that makes their distinct explanatory targets explicit. Section 3 develops the LON-based innovation model: landscape generation, LON construction, and walker dynamics. Section 4 characterizes the structural properties of the resulting LON. Section 5 presents the core results, showing that the model reproduces the main empirical regularities of the discovery-process tradition within a framework that retains the structural features of the adaptive-search tradition, and relates them to the properties of the LON. Section 6 discusses implications for innovation theory, possible empirical strategies, and scope conditions. Section 7 concludes.

## 2 Two Modeling Traditions in Innovation Theory and Their Explanatory Targets

### 2.1 The Discovery-Process Tradition

#### 2.1.1 Empirical targets

The discovery-process literature models innovation records as temporally ordered sequences of tokens drawn from an evolving set of types. Depending on the empirical setting, tokens may be words, scientific concepts, patents, technologies, songs, hashtags, or other items whose first appearance can be identified. A useful general distinction is between *local novelty*, meaning new to a focal sequence or agent, and *system-level novelty*, meaning new to the whole interacting system. This distinction matters in multiagent settings, where something can be novel for one actor without being globally new (Aletti et al., 2023).

Four empirical regularities are central in this tradition.

**Heaps’ law (novelty growth).** Let  $D(t)$  denote the number of distinct items observed after  $t$  draws. In many empirical systems, one finds

$$D(t) \sim t^\beta, \quad 0 < \beta < 1, \quad (1)$$

so that the number of distinct observed types grows sublinearly with sequence length. The interpretation is that novelty continues to appear, but at a decelerating rate. Sublinear growth is often treated as the baseline empirical signature of innovation in temporally ordered records (Tria et al., 2014, 2018).

**Zipf’s law (reuse concentration).** Let  $f(R)$  denote the frequency of a basin of a technology having rank  $R$ . In many innovation-related data sets, the frequency–rank relation is heavy tailed and is often approximated by

$$f(R) \sim R^{-\alpha}. \quad (2)$$

The exponent  $\alpha$  summarizes how concentrated reuse is among previously discovered elements. In idealized cases, the Heaps and Zipf exponents satisfy the reciprocal relation  $\alpha \approx 1/\beta$ , but empirical deviations are common and can reflect correlations, nonstationarity, and finite-size effects (Tria et al., 2014, 2018).

**Taylor’s law (fluctuation scaling).** Let  $n_\Delta(t)$  be the number of innovation events in a time window  $[t, t + \Delta)$ . Across many systems, the variance of  $n_\Delta$  scales as a power of its mean:

$$\text{Var}(n_\Delta) \sim \mathbb{E}[n_\Delta]^\gamma. \quad (3)$$

The benchmark  $\gamma = 1$  corresponds to Poisson-like fluctuations, while  $\gamma > 1$  indicates clustered activity and stronger-than-Poisson variability. Recent work on innovation processes argues that Taylor’s law should be treated not as an optional add-on to Heaps and Zipf, but as a coequal empirical constraint on any adequate generative model (Tria et al., 2018, 2020).

**Inter-event time distribution (burstiness).** Let  $\tau$  denote the time between consecutive novelty events, that is, the inter-event or inter-discovery time. In many empirical systems, the distribution of  $\tau$  follows a heavy-tailed power law:

$$p(\tau) \sim \tau^{-\gamma_{\text{IET}}}. \quad (4)$$

A memoryless (Poisson) discovery process would produce exponentially distributed inter-event times; the empirical observation of power-law tails indicates that discoveries are bursty, arriving in temporally clustered episodes separated by long quiescent intervals (Barabási, 2005; Iacopini et al., 2018). Burstiness is closely related to Taylor’s law: both reflect the same underlying departure from Poisson regularity, but the inter-event time distribution characterizes the temporal fine structure of discovery at the level of individual waiting times rather than windowed counts.

Taken together, these four regularities imply that the discovery-process tradition is concerned not only with how often novelty appears, but also with how novelty, reuse, fluctuations, and temporal clustering are jointly organized over time.

### 2.1.2 Mechanistic families

The discovery-process literature can be organized as a sequence of increasingly structured model families. The simplest starting point is the species-sampling family, including Blackwell–MacQueen, Dirichlet, and Poisson–Dirichlet schemes, in which the probability of seeing an old type is proportional to how often it has appeared before and the probability of a new type is governed by an innovation term. These processes provide an analytically tractable baseline for preferential reuse and sublinear novelty growth, but the space of possibilities is not itself history dependent (Blackwell and MacQueen, 1973; Pitman and Yor, 1997).

A major step beyond exchangeable species-sampling models is to let novelty expand the space of future novelties. This is the core idea of the adjacent possible, formalized in the urn model with triggering and related variants, where the appearance of a novelty introduces further latent possibilities and the opportunity set becomes endogenous to past discoveries. This class of models can generate Heaps’ and Zipf’s laws within a common mechanism and, in later work, Taylor’s law as well (Tria et al., 2014, 2018). Discovery models need not treat the possibility space as an unstructured urn, however. An alternative is to represent concepts as nodes of a graph and model discovery as a reinforced walk, so that semantic locality and temporal correlations emerge because walkers preferentially reuse previously traversed edges while still discovering new nodes (Iacopini et al., 2018).

More recent work makes the discovery process explicitly social: multiple agents explore a space of possibilities while interacting on a social network, so that one agent’s discoveries affect the future discoveries of others. The adjacent possible thereby acquires a social dimension alongside its semantic one, since an actor’s network position shapes the ideas or objects to which they become exposed (Iacopini et al., 2020). A further development is the move away from strictly stationary power-law urns. Damped innovation models modify the update function for old items to fit curved rank–frequency plots and different discovery regimes, while time-dependent urns allow reinforcement and triggering to vary over time or with the number of discovered types, broadening the tradition from canonical power laws to a more general account of how innovation records bend, cross over, or saturate (Aletti and Crimaldi, 2021; Bellina et al., 2025). The newest strand explicitly models several innovation processes that mutually influence one another, distinguishing node-level discoveries from system-level novelties and developing asymptotic and inferential tools for estimating interaction strengths (Aletti et al., 2023, 2025).

Even in its richer networked and interacting forms, the discovery-process tradition primarily models the appearance, recurrence, and correlation of novelties. It rarely endogenizes a performance ordering over states, the basin geometry around locally superior solutions, or the barrier structure that separates incremental improvement from genuine escape. Those are the issues on which adaptive-search models remain especially informative.

## 2.2 The Adaptive-Search Tradition

### 2.2.1 Landscape structure and search

The adaptive-search tradition represents innovation as movement on a performance landscape. A configuration  $s$  in a design space  $\mathcal{S}$  is associated with a performance value  $f(s)$ ,

and search consists of moving through  $\mathcal{S}$  by proposing and evaluating alternative configurations. This approach goes back to the landscape metaphor in evolutionary theory and entered organization and innovation research through NK-style models of interdependent choices (Wright, 1932; Kauffman, 1993; Levinthal, 1997).

In the canonical NK model, ruggedness increases with the degree of interdependence among choices, making local hill climbing more likely to end at a suboptimal peak. But the literature has long moved beyond a single scalar view of complexity. Review work now treats rugged search as a family of problems that vary in decomposability, modularity, hierarchy, cognitive representability, and the possibility of distributed or sequential search (Baumann et al., 2019; Frenken, 2006b). Several structural features recur across this work. Interdependence generates multiple peaks and valleys, making myopic search path dependent; basins of attraction determine where local search is likely to end up, while the distribution of local optima shapes the trade-off between reliable local improvement and the risk of getting trapped (Levinthal, 1997; Kauffman, 1993). The difficulty of search depends not only on how many interdependencies there are, but on how they are organized: near-decomposable or modular architectures permit partial problem decomposition, whereas hierarchical or asymmetric structures make some choices more influential than others (Frenken, 2006a; Ethiraj and Levinthal, 2004; Baumann et al., 2019). It is also important to note that the path dependence generated by fitness-landscape models, where local search trajectories depend on initial conditions and the sequence of moves on a fixed landscape, is analytically distinct from the market lock-in studied in increasing-returns adoption models, where payoffs themselves change through cumulative adoption (Frenken, 2006a,b).

### 2.2.2 Search processes and organizational settings

The adaptive-search literature is not only about landscape structure; it is also about how search is organized. A central issue is whether search is local and incremental or involves long jumps that change multiple choices at once: broader search can help escape low peaks, but it can also waste resources or abandon promising improvements too early (Baumann et al., 2019). Experimental work further shows that search behavior adapts to performance feedback, with success narrowing search to the local neighborhood and repeated failure inducing more exploratory moves (Billinger et al., 2014). Search is often distributed across multiple actors, whether organizational units solving interdependent subproblems or upstream and downstream firms innovating in the same ecosystem; the structure of technological interdependence and input–output flows jointly shape the returns to narrow optimization versus mixing and matching (Ganco et al., 2020). Several extensions abandon the assumption of a fixed landscape entirely: dynamic NK models with environmental turbulence show that broader search becomes relatively more valuable when the environment changes rapidly or extensively, bringing the adaptive-search tradition closer to the temporal concerns of discovery-process models (Li et al., 2019).

Adaptive-search models richly describe how landscape structure and search rules affect performance trajectories, but they do not usually take the empirical regularities of realized innovation records as primary targets. They typically measure adaptation by performance improvement, reached peaks, or time to convergence rather than by the statistics of the resulting innovation sequence.

## 2.3 Local Optima Networks as a Family of Bridge Representations

Local Optima Networks (LONs) compress a fitness landscape into a directed, weighted graph whose nodes are local optima and whose edges represent transition relations between them (Ochoa et al., 2008, 2014). Foundational work defined two main edge semantics. In *basin-transition* LONs, edge weights approximate the probability that a move from one basin of attraction reaches another basin. In *escape-edge* LONs, edges record the probability that a bounded perturbation followed by local search escapes one optimum and reaches another (Vérel et al., 2011). These constructions already showed that LON metrics such as the number of local optima, path length to the global optimum, clustering, modularity, and weight disparity are informative about search difficulty and can correlate with heuristic performance (Chicano et al., 2012; Ochoa et al., 2014).

A key lesson from later work is that there is no single canonical LON. Different construction procedures preserve different aspects of the landscape. Markov-chain sampling records adaptive walks on the local-optima level, whereas snowball sampling recursively explores local-optima neighborhoods from a branching random walk. These two samplers can produce quite different network summaries of the same problem instance, and their features can be complementary rather than substitutable (Thomson et al., 2020). In that sense, a LON should be understood not as one graph but as a family of coarse-grainings defined by a choice of nodes, edges, and sampling rule.

This point is reinforced by method-induced LONs. In memetic differential evolution, for example, parent-child relations between local optima discovered during the run can themselves define a growing weighted network, and network centrality can then be used online to guide future parent selection (Homolya and Vinkó, 2020, 2019). Such constructions do not only summarize a landscape; they summarize how a particular heuristic actually discovers that landscape. This distinction between structural LONs and trace-induced LONs is useful for innovation modeling, where observed innovation records may reveal the latter more readily than the former.

Recent applications also show that neutrality and representation choice can be substantive. In parameter-landscape analysis, monotonic and compressed monotonic LONs collapse equal-fitness plateaus and distinguish optimal from suboptimal sinks, revealing that parameter spaces may be much more multimodal than previous slice-based analyses suggested (Cleghorn and Ochoa, 2021). In feature selection, compressed monotonic LONs identify neutral plateaus among global optima, and these plateaus can reveal irrelevant features directly (Mostert et al., 2019). In AutoML search spaces, varying neighborhood size and perturbation radius changes the number of basins, sinks, and effective distances between optima, showing that search difficulty depends strongly on how local reachability is defined (Teixeira and Pappa, 2022). In morpho-evolution, different encodings of the same task induce markedly different LONs: some show self-loops and short chains, while others generate longer improving trajectories and greater ability to escape poor local optima (Thomson et al., 2024).

These developments are especially important for innovation theory. They imply that a LON is not merely a generic network layered on top of innovation data. It is a coarse-graining of the performance landscape itself, but one whose exact form depends on substantive modeling choices. This makes LONs attractive as a bridge between adaptive-

search models and discovery-process models. On the one hand, they retain information about basins, barriers, sinks, neutrality, community structure, and escape. A stochastic process on a LON generates an innovation record whose novelty growth, revisit concentration, waiting-time structure, and burstiness can be studied directly.

For the purposes of this paper, one concept is particularly useful: *navigability*. By navigability we mean the ease with which search both escapes local optima and continues to discover distinct, high-performing regions of the state space. This extends the usual focus on ruggedness alone and gives a more precise language for relating LON structure to observed innovation dynamics.

## 3 The LON-Innovation Model

Our model consists of three integrated components: (1) a toroidal (periodic boundary condition) fitness landscape representing the space of technological configurations and their performance levels; (2) a Local Optima Network extracted from the landscape and representing its macroscopic structure; and (3) a walker dynamics model representing how innovating agents navigate the LON over time.

### 3.1 Fitness Landscape Generation

#### 3.1.1 Conceptual framework

A fitness landscape is a mapping from a configuration space to a performance measure. In the innovation context, configurations represent technological designs, organizational routines, or strategic positions; performance measures profitability, efficiency, or market share.

We work with a discrete two-dimensional configuration space  $\mathcal{S} = \{0, 1, \dots, L - 1\}^2$ . The two-dimensional case preserves all key qualitative features (multiple optima, basins, communities, ruggedness variation) while enabling visualization and tractable analysis. Extensions to higher dimensions are discussed in Section 6.

**Definition 1** (Fitness Landscape). *A fitness landscape is a tuple  $\mathcal{L} = (\mathcal{S}, f, \mathcal{N})$  where:  $\mathcal{S}$  is the configuration space;  $f : \mathcal{S} \rightarrow \mathbb{R}$  is the fitness function; and  $\mathcal{N} : \mathcal{S} \rightarrow 2^{\mathcal{S}}$  is the neighborhood structure defining which configurations are reachable via incremental innovation.*

#### 3.1.2 Toroidal topology

A critical design choice concerns the boundary conditions of the landscape. Standard reflecting or absorbing boundaries introduce artifacts: artificial barriers or traps at the edges. We impose instead *periodic* (toroidal) boundary conditions:

**Definition 2** (Toroidal Configuration Space). *The toroidal configuration space  $\mathcal{S}_T$  is defined such that  $(x + L, y) \equiv (x, y)$  and  $(x, y + L) \equiv (x, y)$  for all  $(x, y)$ . The toroidal distance between two points is:*

$$d_T((x_1, y_1), (x_2, y_2)) = \sqrt{\min(|x_1 - x_2|, L - |x_1 - x_2|)^2 + \min(|y_1 - y_2|, L - |y_1 - y_2|)^2} \quad (5)$$

The toroidal structure represents an innovation environment without privileged positions: no configuration is inherently central or peripheral, consistent with the abstract, theory-building purpose of the model.

### 3.1.3 Perlin noise generation via the Clifford torus

We generate the fitness function  $f$  using fractional Brownian motion (fBm) built from four-dimensional Perlin noise (Perlin, 1985). The key technical challenge is ensuring that the noise tiles seamlessly on the torus. We solve this by mapping the two-dimensional grid onto a four-dimensional Clifford torus:

**Definition 3** (Clifford Torus Mapping). *The mapping  $\phi : [0, 1)^2 \rightarrow \mathbb{R}^4$  is:*

$$\phi(u, v) = (\cos(2\pi u), \sin(2\pi u), \cos(2\pi v), \sin(2\pi v)) \quad (6)$$

where  $(u, v) = (x/L, y/L)$ . *Adjacent points on the 2D grid (including across boundaries) map to adjacent points in 4D space, guaranteeing seamless tiling.*

**Definition 4** (fBm Fitness Function). *The fitness function with  $n$  octaves is:*

$$f(x, y) = \sum_{i=0}^{n-1} \rho^i \cdot \eta \left( \phi \left( \frac{x}{L}, \frac{y}{L} \right) \cdot \lambda^i \cdot \omega \right) \quad (7)$$

where  $\eta$  is a 4D Perlin noise function;  $\omega$  is the base frequency;  $\lambda$  is the lacunarity (frequency multiplier per octave);  $\rho \in (0, 1)$  is the persistence (amplitude multiplier per octave); and  $n$  is the number of octaves.

The persistence parameter  $\rho$  is the primary control for landscape ruggedness. Low  $\rho$  down-weights high-frequency octaves, producing smooth landscapes with few local optima and large basins. High  $\rho$  gives high-frequency components near-equal weight, producing rugged landscapes with many local optima and small basins. This provides a continuous analog to the epistasis parameter  $K$  in NK landscapes, with a direct interpretation:  $\rho$  controls the degree to which fine-grained technological details interact with coarse-grained design choices.

The final landscape is normalized to  $[0, 100]$ :

$$F(x, y) = 100 \cdot \frac{f(x, y) - f_{\min}}{f_{\max} - f_{\min}} \quad (8)$$

## 3.2 Local Optima and Basins of Attraction

### 3.2.1 Neighborhood and local optima

The neighborhood structure  $\mathcal{N}$  defines the set of configurations reachable from any given point by a single incremental innovation step. We use the *von Neumann* (4-connected) neighborhood, where the neighbors of  $(x, y)$  are the four cardinal-direction points  $(x \pm 1, y)$  and  $(x, y \pm 1)$ , representing constrained innovation where only one attribute of the configuration is modified at a time. The neighborhood is computed modulo  $L$  to respect toroidal boundary conditions.

**Definition 5** (Local Optimum). *A configuration  $s^* \in \mathcal{S}$  is a local optimum if  $f(s^*) \geq f(s)$  for all  $s \in \mathcal{N}(s^*)$ . The global optimum is the local optimum with highest fitness.*

Local optima represent stable technological configurations from which no incremental modification improves performance. An agent that has converged to such a configuration via incremental search exhibits technological lock-in: it cannot improve through any marginal adjustment available within its neighborhood.

### 3.2.2 Hill climbing and optimum identification

Local optima are identified via *steepest-ascent hill climbing*, a deterministic local search procedure that also defines the basin structure of the landscape.

**Definition 6** (Steepest-Ascent Hill Climbing). *Starting from an initial configuration  $s_0 \in \mathcal{S}$ , the hill climbing procedure generates a sequence  $s_0, s_1, s_2, \dots$  by the update rule:*

$$s_{t+1} = \arg \max_{s \in \{s_t\} \cup \mathcal{N}(s_t)} f(s) \quad (9)$$

*The sequence terminates at the first  $t^*$  such that  $s_{t^*+1} = s_{t^*}$ , i.e., when no neighbor improves upon the current configuration. The terminal state  $s^* = s_{t^*}$  is a local optimum.*

Each step selects the single best-improving neighbor, making the ascent greedy and deterministic. The toroidal topology ensures that the neighborhood is well-defined everywhere, with no boundary artifacts. The procedure always terminates in finite time because fitness is bounded and strictly increases at each non-terminal step.

Steepest-ascent hill climbing, as opposed to first-improvement variants, is the natural choice here because it is fully deterministic: every starting point maps to exactly one terminal optimum, making the basin of attraction well-defined and uniquely computable without stochastic runs. This is essential for the LON construction in Section 3.3, which requires a clean partition of the configuration space into non-overlapping basins.

To identify the complete set of local optima in a landscape of size  $L \times L$ , we apply hill climbing exhaustively from every grid point. Each starting location yields a terminal optimum; duplicate results, that is, pairs of identified optima within a small positional tolerance  $\epsilon$  of one another, to account for gradient ties on the discrete grid, are merged by retaining the higher-fitness representative. The final result is a de-duplicated list of local optima  $\{s_1^*, \dots, s_n^*\}$  sorted by decreasing fitness.

### 3.2.3 Basins of attraction

**Definition 7** (Basin of Attraction). *The basin of attraction  $B(s^*)$  of a local optimum  $s^*$  is the set of all configurations from which steepest-ascent hill climbing converges to  $s^*$ :*

$$B(s^*) = \{s \in \mathcal{S} : \text{HillClimb}(s) = s^*\} \quad (10)$$

*The basin size  $|B(s^*)|$  measures the number of configurations in the space from which  $s^*$  is reachable by incremental improvement.*

Because each grid point converges to exactly one optimum, the basins partition  $\mathcal{S}$  exhaustively and without overlap:

$$\bigcup_{i=1}^n B(s_i^*) = \mathcal{S}, \quad B(s_i^*) \cap B(s_j^*) = \emptyset \text{ for } i \neq j \quad (11)$$

The basin size distribution is a key structural property of the landscape. It governs the probability that an agent initiating random exploration will converge to a given optimum, and therefore shapes the likelihood distribution over which technology the agent will discover. Large basins represent robust, easily discoverable technologies; small basins represent fragile configurations that require precisely directed search to reach.

Basin size also correlates with the self-loop structure of the LON, as formalized in Section 3.3: a larger basin implies that random perturbations from the optimum are more likely to remain within the same basin and return to the same optimum via hill climbing, yielding a higher self-loop weight  $w_{ii}$  and thus stronger path dependence at that configuration.

### 3.2.4 Base frequency and the $\omega L$ ratio

The fitness function is generated via fBm in which the lowest-frequency octave oscillates at frequency  $\omega$ . The natural dimensionless control is the product  $\omega L$ , which counts the number of base-frequency cycles that fit within the grid and therefore determines how many dominant performance peaks are present in the configuration space. Large  $\omega L$  (e.g.,  $\omega L = 600$ ) produces a rich mosaic of hills and valleys with many local optima; small  $\omega L$  (e.g.,  $\omega L = 120$ ) yields a landscape dominated by one or two broad features. Holding  $\omega L$  fixed while scaling both  $\omega$  and  $L$  proportionally changes only the resolution, not the qualitative structure, so we treat  $\omega L$  as the primary control for macro-scale landscape richness.

The distinction between  $\omega L$  and  $\rho$  maps onto a substantively meaningful separation:  $\omega L$  controls how many broad, distinct high-performing approaches exist, while  $\rho$  controls the fine-grained ruggedness within each approach. These two levels are independently calibrated, allowing the model to represent a technology with few broad approaches but many internal traps ( $\omega L$  small,  $\rho$  high), or many competing approaches that are each individually smooth ( $\omega L$  large,  $\rho$  low). Figure 1 illustrates the joint effect across  $4 \times 4 = 16$  representative landscapes.

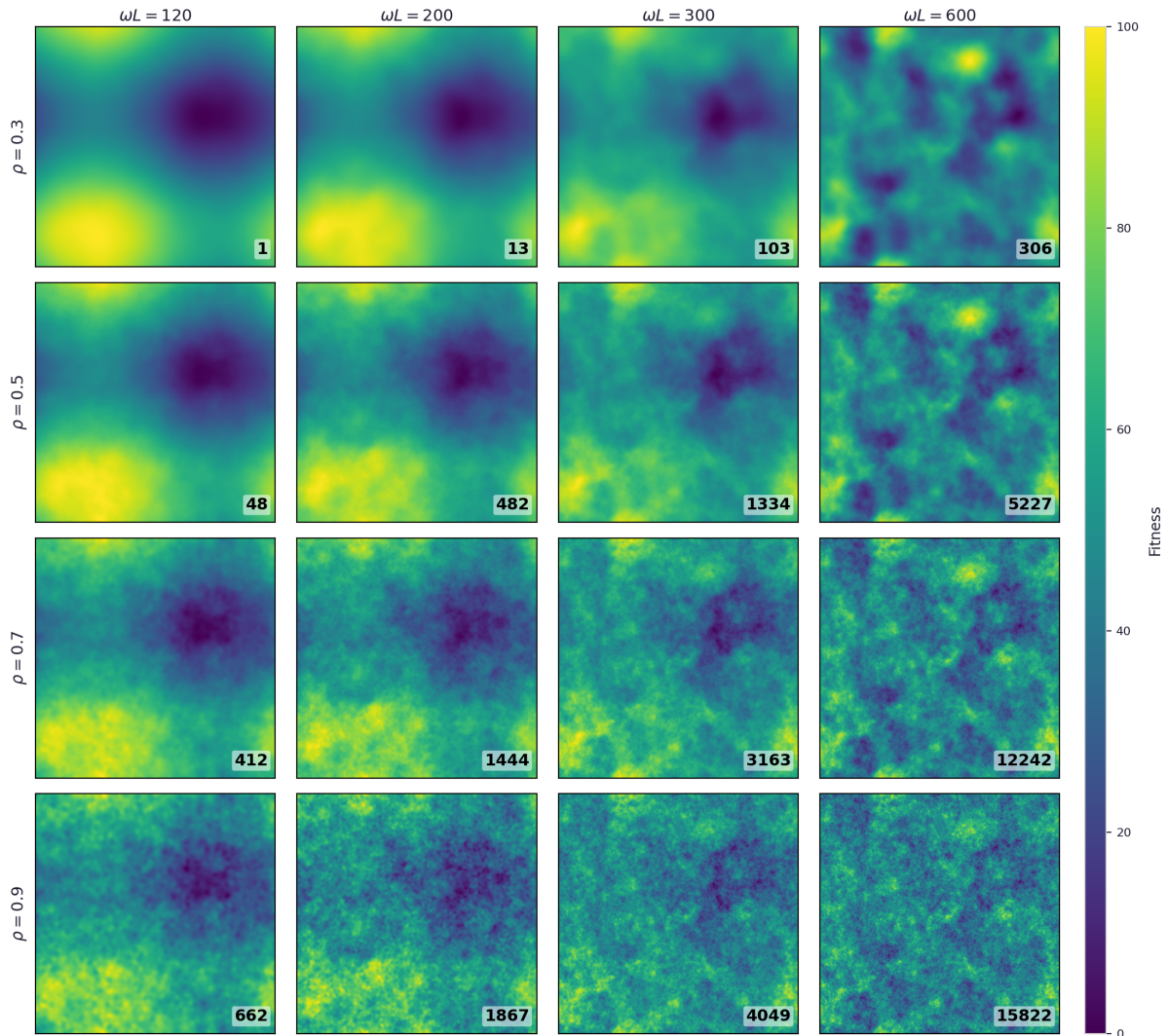


Figure 1: Fitness landscapes varying  $\omega L$  (columns, increasing left to right) and persistence  $\rho$  (rows, increasing top to bottom), with  $L = 1000$  and  $n = 6$  octaves. The number of local optima identified by exhaustive hill climbing is shown in each panel. Fitness is normalized to  $[0, 100]$ .

### 3.3 Local Optima Network Construction

#### 3.3.1 Network definition

**Definition 8** (Local Optima Network). *A Local Optima Network is a directed weighted graph  $G = (V, E, w)$  where nodes  $V = \{v_1, \dots, v_n\}$  represent local optima; edges  $E \subseteq V \times V$  represent possible transitions between basins; and weights  $w : E \rightarrow [0, 1]$  are transition probabilities. Each node  $v_i$  carries attributes: position  $(x_i, y_i)$ , fitness  $f_i = F(x_i, y_i)$ , and basin size  $|B(v_i)|$ .*

Figure 2 illustrates the relationship between a fitness landscape and its corresponding LON for a representative parameter configuration. The left panel shows the landscape with its local optima marked as stars; the right panel shows the resulting LON, where nodes are positioned at their spatial coordinates in the landscape, node color encodes fitness, and directed edges encode inter-basin transitions. Self-loop edges, that is, transi-

tions from a node back to itself representing perturbations that remain within the same basin, are not shown; for many nodes, particularly those sitting atop the broad high-fitness hills, the self-loop weight  $w_{ii}$  is the dominant outgoing weight. Several edges span what appears to be the full width or height of the panel, connecting nodes on opposite sides of the grid; these are not anomalous long-range connections but a direct consequence of the toroidal topology, in which the left and right borders are identified and the same holds for top and bottom.

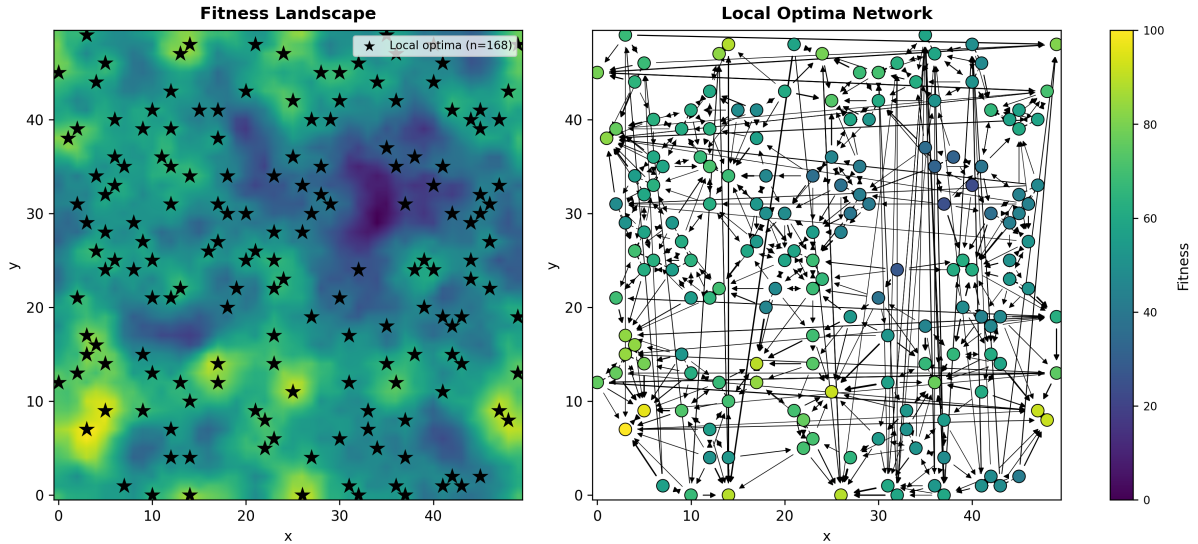


Figure 2: Left: a representative fitness landscape with local optima marked as stars. Right: the corresponding Local Optima Network, with nodes positioned at their landscape coordinates and colored by fitness  $f_i$  (same colormap). Directed edges represent inter-basin transitions with probability  $w_{ij} > 0$ ; self-loops ( $w_{ii}$ ) are omitted for clarity. Edges that cross the boundary of the panel connect nodes that are spatially adjacent on the torus.

### 3.3.2 Weighted edge construction via basin-hopping

We construct edges using a *basin-hopping* procedure. From each optimum  $v_i$ , we sample  $m$  random initial points uniformly from the ball of radius  $r$  centered at  $v_i$ , apply hill climbing to each of them, and record which basin is reached. The edge weight  $w_{ij}$  is the fraction of points around  $v_i$  that converge to  $v_j$ :

$$w_{ij} = \frac{1}{m} \sum_{k=1}^m \mathbf{1}[\text{HillClimb}(v_i + \delta_k) = v_j], \quad \delta_k \sim \text{Uniform}([-r, r]^2) \quad (12)$$

Weights are normalized so that outgoing edges from each node sum to one:

$$\sum_{j:(i,j) \in E} w_{ij} = 1 \quad \forall i \in V \quad (13)$$

The weight  $w_{ij}$  has a direct interpretation: it is the probability that an agent at local optimum  $i$ , upon experiencing a random perturbation within radius  $r$ , will be directed to

optimum  $j$  by subsequent hill climbing. The self-loop weight  $w_{ii}$  measures basin robustness, the probability that the agent returns to its current configuration after perturbation, while the escape probability  $1 - w_{ii}$  measures the ease of transitioning to a different locally stable technological approach.

### 3.3.3 Perturbation radius and the characteristic inter-optimum distance

The perturbation radius  $r$  is the most consequential structural parameter of the LON construction. It determines not only the weights on individual edges but the global connectivity of the network. To set  $r$  in a principled way, we define the *characteristic inter-optimum distance*:

$$d^* = \frac{L}{\sqrt{n}} \quad (14)$$

where  $n$  is the number of local optima. This quantity is not a free parameter but an emergent property of the landscape: since  $n$  is determined by  $\omega L$  and  $\rho$ ,  $d^*$  decreases as landscapes become more rugged and increases as they become smoother.

The ratio  $r/d^*$  governs a percolation transition in the LON's connectivity.<sup>1</sup> When  $r \ll d^*$ , perturbations from any optimum are almost entirely confined within its own basin: the LON consists of isolated self-loops with negligible inter-node edges. When  $r \gg d^*$ , the LON is densely connected and the fitness-correlated heterogeneity that gives the network its innovation-theoretic content is progressively destroyed.

In the baseline model, we fix  $r \approx d^*$ . This is the regime of richest structure and most sensitive dynamics: the network is globally connected but sparse, with high-fitness broad-basin nodes retaining high self-loop weights while low-fitness narrow-basin nodes provide the connective tissue. Increasing  $r$  above  $d^*$  erodes the self-loop dominance of even the highest-fitness nodes and broadens the out-degree distribution, moving the walk toward uniform mixing; decreasing  $r$  below  $d^*$  fragments the network into isolated components, trapping agents at their initial optima.

## 3.4 Walker Dynamics Model

### 3.4.1 The walker as an innovating agent

An innovating agent, whether a firm, research team, or inventor, is modeled as a stochastic walker on the LON. The walker's state  $v_t \in V$  at time  $t$  is the local optimum it currently occupies.

**Definition 9** (LON Walker). *A walker on LON  $G = (V, E, w)$  is characterized by its current node  $v_t$  and the Markov transition rule:*

$$\Pr(v_{t+1} = j \mid v_t = i) = w_{ij} \quad (15)$$

*The walker's fitness history  $\{f_{v_0}, f_{v_1}, \dots\}$  and novelty record  $\{t : v_t \notin \{v_0, \dots, v_{t-1}\}\}$  are the primary observables.*

Each step represents a period of incremental exploration, after which the agent either returns to the same configuration (reflecting the basin's robustness) or transitions to

---

<sup>1</sup>According to our experience and the parameter space that we explored, the percolation transition happens at around  $r/d^* = 0.25$

a neighboring basin (if the perturbation exceeds the basin boundary). The self-loop weight  $w_{ii}$  directly controls the probability of remaining in the current configuration, operationalizing path dependence.

### 3.4.2 Innovation record and novelty events

From the walker’s trajectory, we define two key observables that connect to the discovery process literature:

**Definition 10** (Novelty Rate and Revisit Rate). *Let  $\mathcal{V}(t) = \{v_0, v_1, \dots, v_t\}$  be the set of distinct optima visited by time  $t$ . The novelty count is  $D(t) = |\mathcal{V}(t)|$ . The visit frequency of optimum  $v$  is  $n_v(t) = |\{\tau \leq t : v_\tau = v\}|$ .*

The novelty count  $D(t)$  is the direct analog of the distinct-item count in urn models. Its growth rate determines whether the walk exhibits Heaps-like behavior. The visit frequency distribution  $\{n_v(t)\}_{v \in \mathcal{V}(t)}$  is the analog of the rank-frequency distribution in Zipf’s law. The sequence of times at which new optima are first visited defines the inter-event time series whose distribution is the analog of the burstiness signature in Equation (4).

### 3.4.3 Exogenous innovation: A further escape mechanism

The baseline model as described above is driven entirely by the basin-hopping dynamics encoded in the transition weights  $w_{ij}$ , i.e., by endogenous innovations. As shown in Section 5, this is sufficient to generate all four empirical regularities. The model can, however, be augmented with a small probability  $\varepsilon > 0$  of teleporting to a uniformly random node at each step:

$$\Pr(v_{t+1} = j \mid v_t = i) = (1 - \varepsilon) w_{ij} + \frac{\varepsilon}{n} \quad (16)$$

This teleportation represents a rare exogenous event, such as an external technology transfer or a recombination insight, that places the agent in a region of the configuration space unreachable by incremental search. For any  $\varepsilon > 0$ , Equation (16) defines an ergodic Markov chain with a unique stationary distribution over all  $n$  nodes. The effects of introducing a small  $\varepsilon$  on the four innovation exponents are explored in Section 5.7.

## 3.5 Model Parameters

Table 1 provides a complete summary of the model’s parameters, organized by the component in which they appear. The landscape is characterized by the base frequency  $\omega$  and grid size  $L$ , whose product  $\omega L$  controls the macro-scale richness of the performance surface together with persistence  $\rho$ , which governs fine-scale ruggedness. The LON construction is determined by the neighborhood type  $\mathcal{N}$  and perturbation radius  $r$ , the latter fixed at the characteristic inter-optimum distance  $d^* = L/\sqrt{n}$ . Walker dynamics are fully determined by the basin-hopping transition weights in the baseline ( $\varepsilon = 0$ ); the optional exogenous innovation rate  $\varepsilon$  can be set to a small positive value to introduce rare random jumps.

Table 1: Model parameter summary.

Component	Parameter	Symbol	Interpretation
Landscape	Grid size	$L$	Resolution of the configuration space
	Base frequency	$\omega$	Spatial scale of dominant features; $\omega L$ counts feature cycles across the grid
	Persistence	$\rho$	Fine-scale ruggedness; high $\rho$ yields many optima with small basins
	Octaves	$n$	Number of superimposed frequency layers
LON construction	Neighborhood	$\mathcal{N}$	Incremental move set (von Neumann, 4-connected)
	Perturbation radius	$r$	Reach of non-incremental search; fixed at $d^* = L/\sqrt{n}$
	Perturbation samples	$m$	Number of random draws per node for edge weight estimation
Walker	Exogenous innovation	$\varepsilon$	Probability of teleporting to a uniformly random node at each step; $\varepsilon = 0$ in the baseline

## 4 Structural Properties of the Local Optima Network

The LON constructed in Section 3.3 is not merely a convenient summary of the landscape: its topology encodes the full set of constraints on how an innovating agent can move through the space of locally stable technological approaches. Before turning to walker dynamics and the resulting innovation records, it is worth characterizing the structural properties that emerge from the construction itself.

### 4.1 Fitness, Self-Loop Weight, and Incoming Degree

Three node attributes are of central importance: the fitness  $f_i$  of the optimum, its self-loop weight  $w_{ii}$ , and its weighted incoming degree  $k_i^{\text{in}} = \sum_{j \neq i} w_{ji}$ . These three quantities are not independent: they are jointly determined by basin geometry in ways that have direct implications for innovation dynamics.

#### 4.1.1 Fitness and self-loop weight

**Proposition 1** (Fitness–Self-Loop Correlation). *In fBm landscapes with persistence  $\rho < 1$ , fitness and self-loop weight are positively correlated:*

$$\text{Corr}(f_i, w_{ii}) > 0 \tag{17}$$

High-fitness optima in fBm landscapes sit atop broad, smooth hills where the low-frequency octaves dominate. A random perturbation of radius  $r$  from such a peak is

likely to land on the same slope and be returned to the same optimum by hill climbing, yielding high  $w_{ii}$ . Low-fitness optima, by contrast, arise from constructive interference of high-frequency octaves, producing narrow basins from which perturbations easily escape. This correlation is the LON-theoretic foundation of path dependence: high-performing technological approaches are inherently more stable, and an agent that has found one will tend to return to it repeatedly. The reinforcement arises endogenously from basin geometry rather than being imposed as a modeling assumption.

#### 4.1.2 Fitness and incoming degree

The weighted incoming degree  $k_i^{\text{in}} = \sum_{j \neq i} w_{ji}$  measures the total probability flux arriving at  $v_i$  from all other nodes in a single perturbation step.

**Proposition 2** (Fitness–Incoming Degree Correlation). *In fBm landscapes, fitness and weighted incoming degree are positively correlated:*

$$\text{Corr}(f_i, k_i^{\text{in}}) > 0 \quad (18)$$

Larger basins present a larger cross-section to perturbations from neighboring optima and therefore accumulate higher incoming weight from more sources. Since basin size is positively correlated with fitness by the same geometric argument as in Proposition 1, fitness and incoming degree inherit the same positive correlation. High-fitness nodes are therefore simultaneously hard to escape (high  $w_{ii}$ ) and easy to fall into (high  $k_i^{\text{in}}$ ), so that the stationary distribution of a random walk on the LON is concentrated on high-fitness nodes.

Figure 3 illustrates these relationships for the baseline LON used throughout Section 5 ( $\rho = 0.8$ ,  $n = 7$ ,  $\omega L = 600$ ). The left panel shows fitness against self-loop weight ( $r_S = 0.224$ ): the positive trend is present but noisy. The centre panel shows fitness against weighted incoming degree ( $r_S = 0.257$ ): the trend is steeper and more structured. The right panel shows fitness against expected sojourn time  $\bar{t}_i = \pi_i / (1 - w_{ii})$  on a logarithmic axis ( $r_S = 0.523$ ): sojourn times span roughly four orders of magnitude, from  $\sim 10^{-6}$  for the most transient low-fitness nodes to  $\sim 10^{-2}$  for the dominant community attractors, with an approximately log-linear relationship across this range.

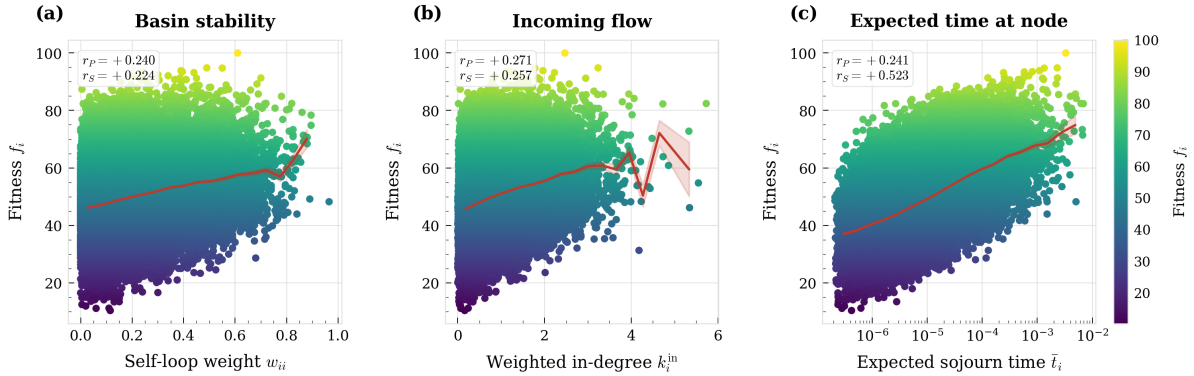


Figure 3: Node-level attribute relationships in the baseline LON ( $\rho = 0.8$ ,  $n = 7$ ,  $\omega L = 600$ ). Left: fitness  $f_i$  versus self-loop weight  $w_{ii}$ . Centre: fitness versus weighted incoming degree  $k_i^{\text{in}} = \sum_{j \neq i} w_{ji}$ . Right: fitness versus expected sojourn time  $\bar{t}_i = \pi_i / (1 - w_{ii})$  (log scale), where  $\pi_i$  is the stationary probability of the random walk. Points are colored by fitness. Red lines show binned means ( $\pm 1$  SE); Pearson ( $r_P$ ) and Spearman ( $r_S$ ) correlations are reported in each panel.

### 4.1.3 The joint structure and its consequences

These relationships form a coherent joint structure. High-fitness nodes are simultaneously large-basin, high self-loop, and high in-degree. They function as the stable attractors of the network: easy to discover, hard to leave, and frequently revisited. Low-fitness nodes, by contrast, sit in narrow basins with low self-loop weights, making them transient way-points from which agents are quickly displaced. The resulting heterogeneity in residence times and visit frequencies is a structural feature of the LON that, as shown in Section 5, directly shapes the Zipf-law exponent and the heavy-tailed character of inter-event times.

## 4.2 Community Structure and Technological Paradigms

The node-level properties examined in Section 4.1 characterize individual optima in isolation. A complementary question concerns the *meso-scale* structure of the LON: how do local optima organize into groups, and what do these groups represent in innovation terms?

We identify communities using the *Walktrap algorithm* (Pons and Latapy, 2006), which groups nodes into clusters within which short random walks tend to remain. The algorithm defines a distance between nodes based on transition probabilities over short walks, then applies hierarchical agglomeration to partition the network. Walktrap is a natural choice here because its underlying dynamics are structurally identical to the walker model of Section 3.4, and because it is sensitive to edge weights, so that the transition probabilities  $w_{ij}$  directly inform community boundaries.

**Definition 11** (Technological Paradigm). *A technological paradigm in the LON model is operationalized as a community  $C_k \subset V$  identified by Walktrap community detection: a set of local optima that are mutually accessible through incremental basin transitions, but from which escape to other communities requires either a rare large perturbation or an exogenous innovation event ( $\varepsilon$ -teleportation). Each community contains a high-fitness attractor node that functions as the community's dominant stable configuration.*

Each community represents a coherent *technological approach*: a family of related designs among which an agent can move fluidly through basin transitions, with dynamics governed by local optimization toward the community’s high-fitness attractor. Crossing a community boundary represents a qualitative reorientation that requires overcoming the inter-community barriers encoded in the LON’s edge structure. This provides a network-grounded operationalization of the concept of technological paradigm as used by Dosi (1982): the community delineates the set of configurations reachable through the paradigm’s characteristic search heuristics, and the community boundary marks where search must either make a large jump or wait for an exogenous event to access a qualitatively different set of solutions.

Figure 4 illustrates the community structure of a representative LON. Communities are roughly spatially cohesive, reflecting that nearby optima tend to be connected by short transitions, but long-range edges produced by toroidal wrapping occasionally link spatially distant optima into the same community. Communities vary substantially in size, with a few large communities dominating and many smaller peripheral ones.

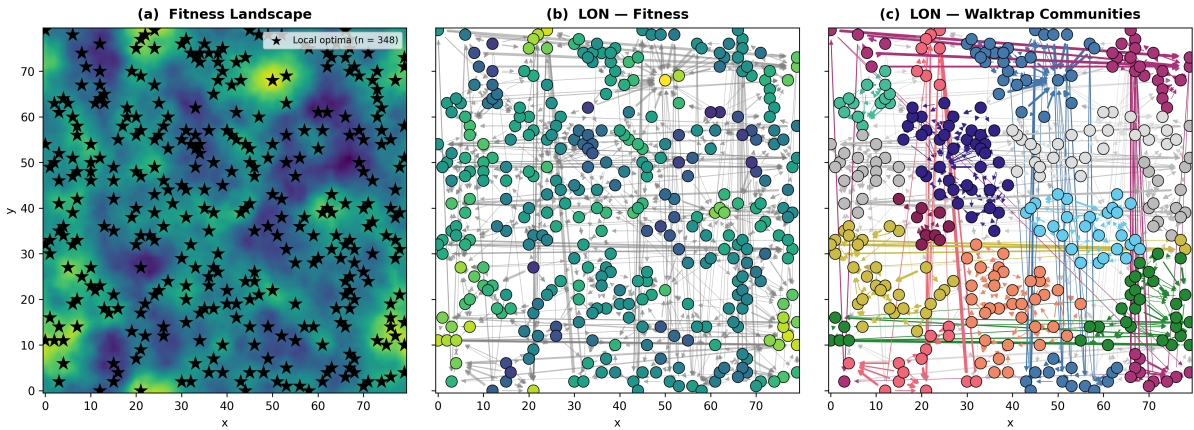


Figure 4: Community structure of a representative LON. (a) Fitness landscape with local optima marked as stars ( $N = 622$ ). (b) LON with nodes colored by fitness  $f_i$ ; edges shown in grey. (c) LON with nodes colored by Walktrap community assignment (Pons and Latapy, 2006). Each color represents a distinct community, interpreted as a technological paradigm: a set of locally stable approaches that are mutually accessible through incremental transitions. Edges crossing community boundaries are shown in the community color of their source node.

The community structure interacts with the node-level properties of Section 4.1 in a systematic way. High-fitness nodes act as community attractors, while low-fitness nodes near community boundaries are the most likely points of inter-community transition. The resulting two-level vocabulary, basins for incremental innovation and communities for technological paradigms, provides the interpretive framework for Section 5: residence within a basin corresponds to exploitation of a specific configuration; movement across basins within a community corresponds to incremental exploration within the current paradigm; and transitions across community boundaries correspond to paradigm shifts.

## 5 Model Capabilities: Replicating Innovation Regularities

This section is the core analytical contribution of the paper. We show how the LON-innovation model generates the four key empirical regularities of the discovery-process tradition, identify the LON structural features responsible for each, and demonstrate how the exponents respond to changes in model parameters.

### 5.1 Baseline Configuration and a Representative Walk

The baseline analysis uses the following parameter configuration: grid size  $L = 1,000$ , base frequency  $\omega = 0.6$  (so that  $\omega L = 600$ ), persistence  $\rho = 0.8$ ,  $n = 7$  octaves, 4-connected neighborhood, perturbation radius  $r = 10$ , and  $m = 200$  perturbation samples per node. The exogenous innovation rate is set to  $\varepsilon = 0$ , so that all exploration is driven entirely by the basin-hopping dynamics of the LON, without any random teleportation.

Before examining ensemble statistics, it is instructive to look at what a single walk on the LON actually produces. Figure 5 shows a trajectory of  $T = 200,000$  steps on a LON with  $|V| = 47,272$  nodes, constructed from the baseline landscape parameters. Panel (a) records the fitness change  $\Delta f = f_{\text{new}} - f_{\text{prev}}$  at each discovery event, that is, each time the walker visits a previously unvisited optimum, where  $f_{\text{prev}}$  is the fitness of the last novel optimum discovered. Two features are immediately apparent. Discovery events are not spread uniformly over time: they cluster into dense bursts, separated by long quiescent intervals during which the walker revisits already-known optima without encountering any new ones. And the fitness changes within each burst are a mix of improvements (red spikes) and regressions (blue spikes), reflecting the fact that the walker does not follow a monotonically improving path through the LON but instead explores heterogeneous neighborhoods in which some new optima have higher fitness than the previous discovery and others have lower.

Panel (b) shows the cumulative number of distinct optima discovered,  $D(t)$ . The trajectory has a characteristic staircase shape: steep risers correspond to the burst episodes visible in panel (a), during which the walker enters a new community or an unexplored region of its current community and discovers many new optima in rapid succession; plateaus correspond to the quiescent intervals during which the walker is trapped at high self-loop nodes and the novelty count is flat. The plateaus grow longer as the walk progresses, because the walker progressively exhausts the easily reachable optima in its vicinity and must traverse increasingly rare inter-community transitions to find new ones.

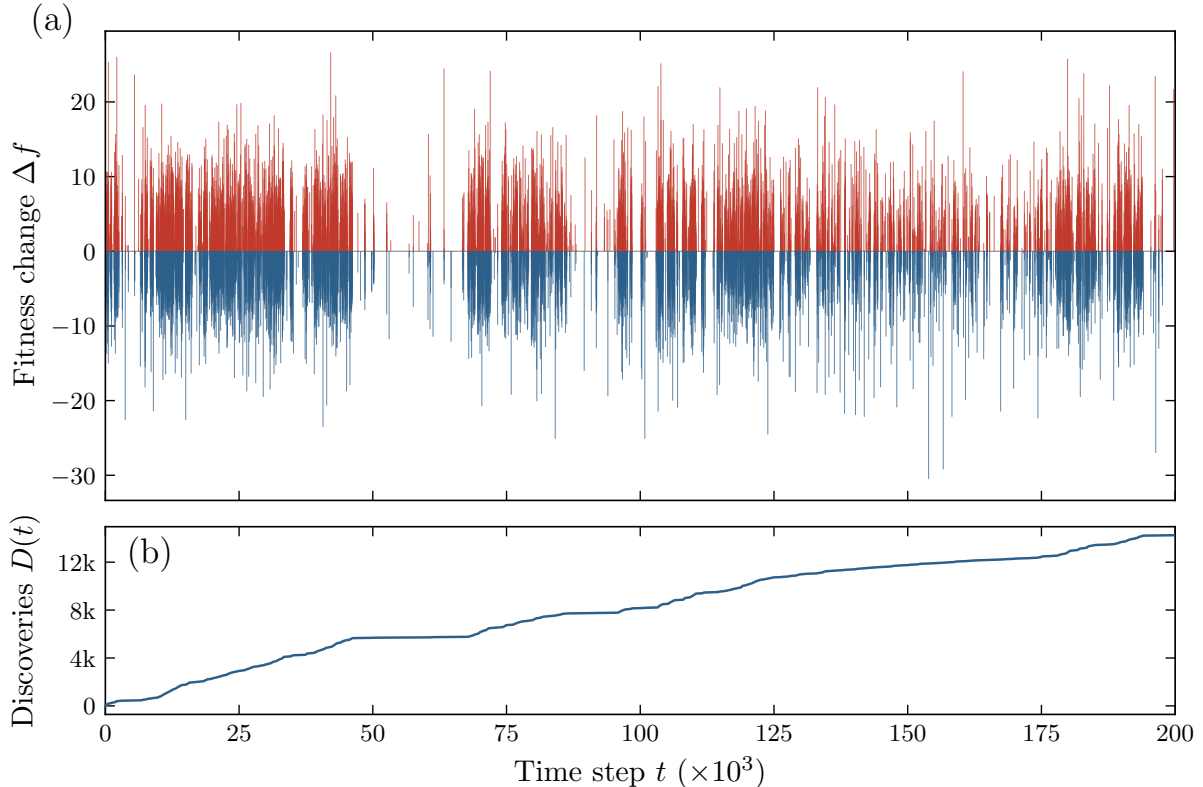


Figure 5: **Punctuated discovery dynamics.** A single walk on the baseline LON ( $|V| = 47,272$  nodes). **(a)** Fitness change  $\Delta f = f_{\text{new}} - f_{\text{prev}}$  at each discovery event. Red (blue) spikes indicate fitness improvements (regressions); events cluster into bursts separated by quiescent intervals. **(b)** Cumulative distinct optima  $D(t)$ . Plateaus correspond to trapping episodes; risers correspond to burst phases.

This punctuated pattern is the single-trajectory signature of the statistical regularities analyzed in the remainder of this section. The staircase shape of  $D(t)$  is what produces sublinear Heaps' law growth when averaged over many replications. The clustering of discoveries into bursts is what produces heavy-tailed inter-event time distributions. And the heterogeneous burst sizes across different communities are what produce Zipf-law concentration in visit frequencies and Taylor-law anomalous fluctuation scaling.

To characterize these regularities quantitatively, we adopt a two-level ensemble design. We generate 20 independent landscapes (and their corresponding LONs) from different random seeds, and for each LON we run 50 independent walker replications of length  $T = 200,000$  steps, yielding a total of 1,000 replications. This design ensures that the reported statistics reflect variation across both the structural properties of different LON realizations and the stochastic trajectories of different walkers on the same LON. Figure 6 summarizes the ensemble results.

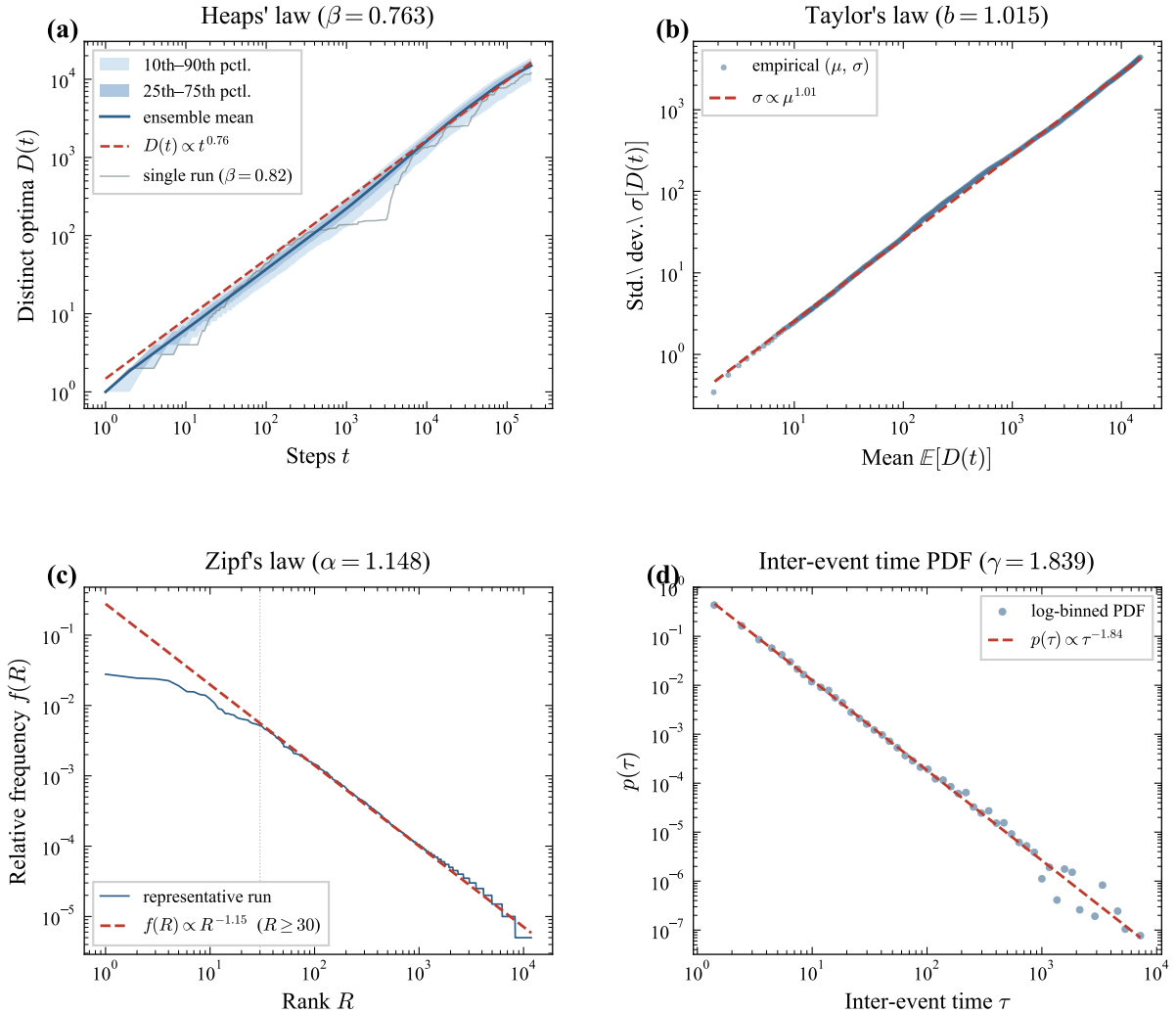


Figure 6: Baseline ensemble results ( $\rho = 0.8$ ,  $n = 7$  octaves,  $\varepsilon = 0$ ; 20 LONs  $\times$  50 walks = 1,000 replications,  $T = 200,000$ ). (a) Heaps' law: distinct optima  $D(t)$  versus step  $t$ , with ensemble mean, percentile bands, and fitted exponent  $\beta = 0.763$ . (b) Taylor's law:  $\sigma[D(t)]$  versus  $\mathbb{E}[D(t)]$ , with fitted exponent  $b = 1.015$ . (c) Zipf's law: rank-frequency distribution (representative run), with tail fit  $\alpha = 1.148$  for ranks  $R \geq 30$ . (d) Inter-event time PDF (representative run), with fitted exponent  $\gamma_{\text{IET}} = 1.839$ .

## 5.2 Heaps' Law: Sublinear Novelty Growth

Figure 6a shows the ensemble-averaged novelty count  $D(t)$ , the number of distinct optima visited by step  $t$ , on log-log axes. The ensemble mean follows a clear power-law regime  $D(t) \sim t^\beta$  with fitted exponent  $\beta = 0.763$ , and a representative single run ( $\beta = 0.82$ ) is shown for comparison. The inner shaded band covers the 25th–75th percentiles; the outer band spans the 10th–90th percentiles across all 1,000 replications.

The sublinear exponent  $\beta < 1$  arises from the interplay between the LON's self-loop structure and its community organization. At early times, the walker is confined to its initial community, where it encounters new optima at a rate governed by the local out-degree and the self-loop weights of the nodes it visits. Because high-fitness nodes have high  $w_{ii}$  (Proposition 1), the walker spends many steps returning to already-visited configurations before escaping to a neighboring basin. This produces a discovery rate that is slower

than linear from the outset. As the walk progresses and the walker exhausts the optima in its current community, further novelty requires crossing a community boundary, which is rare due to the inter-community bottleneck structure. In the baseline configuration, where  $\varepsilon = 0$ , there is no teleportation mechanism to assist escape: the walker must reach a new community entirely through the basin-hopping dynamics. The decreasing marginal rate of novelty production is therefore a direct consequence of the hierarchical trapping structure of the LON: basins within communities, and communities within the network as a whole, create nested barriers to exploration.

The fitted exponent  $\beta = 0.763$  falls within the range commonly reported in empirical innovation data (Tria et al., 2014, 2018). The single-run exponent ( $\beta = 0.82$ ) is somewhat higher, reflecting the greater stochasticity of individual trajectories. The gap between single-run and ensemble exponents is itself informative: it indicates that averaging over multiple LON realizations and their heterogeneous community structures produces a more regular, and somewhat slower, novelty growth curve than any individual realization.

### 5.3 Taylor’s Law: Fluctuation Scaling

Figure 6b shows the Taylor-law relationship between the mean  $\mu$  and standard deviation  $\sigma$  of the cumulative novelty count  $D(t)$  across the ensemble, evaluated at logarithmically spaced time points. The empirical relationship  $\sigma \sim \mu^b$  is fitted with exponent  $b = 1.015$ .

The exponent  $b \approx 1$  indicates that fluctuations in the novelty count scale almost linearly with the mean, placing the model firmly in the stronger-than-Poisson, correlated regime. This is a direct consequence of the two-level heterogeneity built into the ensemble design. At the first level, different LON realizations have different community structures, basin size distributions, and self-loop weight profiles, so that walkers on different LONs face structurally different exploration landscapes. At the second level, walkers on the same LON starting from different initial conditions can become trapped in different communities for extended periods. A walker that arrives early in a large, high-connectivity community discovers many new optima quickly, while a walker trapped in a small community with high self-loop weights at its attractor node discovers new optima slowly. This community-level heterogeneity in discovery rates amplifies the cross-replication variance of  $D(t)$  beyond what a memoryless process would produce.

The Taylor exponent  $b \approx 1$  is consistent with the values reported in empirical studies of innovation records (Tria et al., 2018, 2020) and with the theoretical prediction that correlated, bursty discovery processes produce Taylor exponents near or above unity.

### 5.4 Zipf’s Law: Heavy-Tailed Reuse

Figure 6c shows the rank-frequency distribution of visited optima for a representative run: the relative visit frequency  $f(R)$  of the optimum of rank  $R$  (sorted by decreasing frequency) on log-log axes. The tail of the distribution (ranks  $R \geq 30$ ) follows a power law  $f(R) \sim R^{-\alpha}$  with fitted exponent  $\alpha = 1.148$ .

The Zipf exponent close to unity reflects the concentration of visits on a small number of high-fitness, high self-loop nodes. As established in Section 4.1, high-fitness nodes simultaneously attract large incoming flow ( $k_i^{\text{in}}$  high) and retain walkers for long sojourns ( $w_{ii}$  high). The stationary distribution of the random walk is therefore heavily skewed:

a few community-attractor nodes accumulate a disproportionate share of the total visit mass, while the many low-fitness transient nodes in the network periphery are visited rarely and briefly.

The characteristic shape of the rank-frequency curve, with a flattened head at low ranks and a steeper power-law tail, is a signature of the LON’s joint structure of fitness, self-loop weight, and incoming degree. The top-ranked optima (roughly the top 20–30) correspond to the dominant attractors of the largest communities; their visit frequencies are compressed relative to one another because even without teleportation, the basin-hopping dynamics eventually carry the walker across community boundaries, redistributing some visit mass. Beyond the head, the tail follows the power law: the many small-basin, low-fitness optima that form the periphery of each community are visited with frequencies that decay as a regular function of rank.

## 5.5 Inter-Event Time Distribution: Bursty Discovery Dynamics

Figure 6d shows the probability density function of inter-event times  $\tau$ , where  $\tau$  is the number of steps between consecutive novelty events (first visits to previously unvisited optima), for a representative run. The log-binned empirical density follows a power law  $p(\tau) \sim \tau^{-\gamma_{\text{IET}}}$  with fitted exponent  $\gamma_{\text{IET}} = 1.839$  over more than three orders of magnitude in  $\tau$ .

The heavy-tailed inter-event time distribution is the temporal fingerprint of the LON’s community and trapping structure. Within a community, novelty events can occur in rapid succession as the walker transitions between neighboring basins, producing short inter-event times. Once the walker has visited most optima in its current community, however, further novelty requires a rare inter-community transition through the basin-hopping dynamics alone (since  $\varepsilon = 0$ ). The walker then enters a long quiescent phase during which it revisits already-known optima, producing a long inter-event time. The distribution of these quiescent durations is governed by the distribution of self-loop sojourn times and community escape times, both of which are heavy tailed due to the heterogeneous  $w_{ii}$  distribution across nodes and the heterogeneous community sizes across the LON.

The resulting picture is one of bursty discovery: episodes of rapid novelty production when the walker enters a new community (or a previously unexplored region of its current community), separated by long waiting times during which the walker is trapped at high-fitness attractors. This is the temporal analog of the spatial heterogeneity captured by Zipf’s law: just as visit frequencies are concentrated on a few dominant optima, novelty events are concentrated in temporal bursts rather than spread uniformly over time.

The exponent  $\gamma_{\text{IET}} = 1.839$  falls in the range commonly observed in empirical studies.

## 5.6 Joint Consistency of the Four Regularities

A key feature of the results presented above is that all four regularities emerge simultaneously from the same ensemble of walks on the same set of LONs, without any parameter tuning specific to individual regularities. The exponents are jointly determined by the structural properties of the LON: the distribution of self-loop weights, the community size distribution, and the fitness-degree correlation.

The joint consistency reflects the fact that the LON encodes a single, coherent trapping-and-escape landscape, and the four regularities are simply different projections of the same underlying dynamics. Heaps’ law describes the cumulative count of distinct states; Zipf’s law describes the equilibrium distribution of visits across states; Taylor’s law describes the cross-replication variability of cumulative counts; and the inter-event time distribution describes the temporal fine structure of novelty production. All four are governed by the same competition between within-community exploitation (driven by self-loop weights and community attractors) and cross-community exploration (driven by low-fitness boundary nodes and the basin-hopping dynamics).

## 5.7 Parameter Variations

The baseline configuration is not the only one that produces the four regularities. To illustrate how the exponents respond to changes in model parameters, we consider three variations that each modify a single aspect of the baseline while holding everything else fixed. Table 2 summarizes the four configurations and their fitted exponents; Figures 7 to 9 show the corresponding ensemble panels.

Table 2: Parameter configurations and fitted exponents. All configurations use  $L = 1,000$ , 4-connected neighborhood,  $r = 10$ ,  $m = 200$ ,  $T = 200,000$ , 20 LONs  $\times$  50 walks.

Configuration	$\rho$	$n$	$\varepsilon$	$\beta$	$b$	$\alpha$	$\gamma_{\text{IET}}$
Baseline	0.8	7	0	0.763	1.015	1.148	1.839
Fewer octaves	0.8	6	0	0.650	1.113	1.223	1.492
Higher persistence	0.9	7	0	0.732	1.091	0.950	1.922
Exogenous innovation	0.8	7	$10^{-5}$	0.777	0.990	1.066	1.867

### 5.7.1 Reducing landscape complexity: fewer octaves

Figure 7 shows the ensemble results when the number of octaves is reduced from  $n = 7$  to  $n = 6$ , with all other parameters held at their baseline values. Removing the highest-frequency layer produces a smoother landscape with fewer local optima and larger basins, yielding a LON with fewer nodes, broader basins, and higher average self-loop weights.

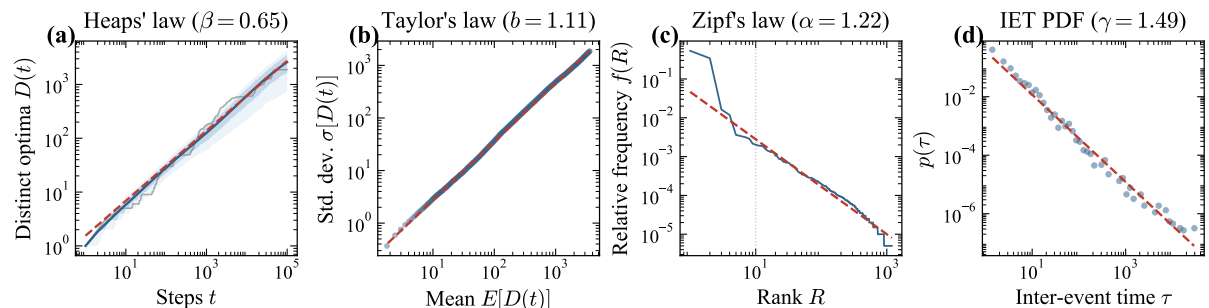


Figure 7: Ensemble results with reduced landscape complexity ( $n = 6$  octaves,  $\varepsilon = 0$ ; all other parameters as in Figure 6). Fitted exponents:  $\beta = 0.650$ ,  $b = 1.113$ ,  $\alpha = 1.223$ ,  $\gamma_{\text{IET}} = 1.492$ .

The consequences are systematic: the Heaps exponent drops to  $\beta = 0.650$  (slower novelty growth due to stronger trapping in broad basins); the Zipf exponent rises to  $\alpha = 1.223$  (more concentrated visits on the fewer dominant attractors); the Taylor exponent rises to  $b = 1.113$  (greater cross-replication variability because the starting community matters more when communities are few); and the inter-event time exponent drops to  $\gamma_{\text{IET}} = 1.492$ , indicating a substantially heavier tail. This last change is the most striking: with fewer and broader basins the self-loop sojourn times at dominant attractors are longer and inter-community transitions are rarer, making the landscape less navigable and quiescent intervals longer.

### 5.7.2 Increasing fine-scale ruggedness: higher persistence

Figure 8 shows the ensemble results when persistence is increased to  $\rho = 0.9$ , with all other parameters at baseline. Higher  $\rho$  up-weights the high-frequency octaves, producing a more rugged landscape with more local optima, narrower basins, and a denser, more heterogeneous edge structure.

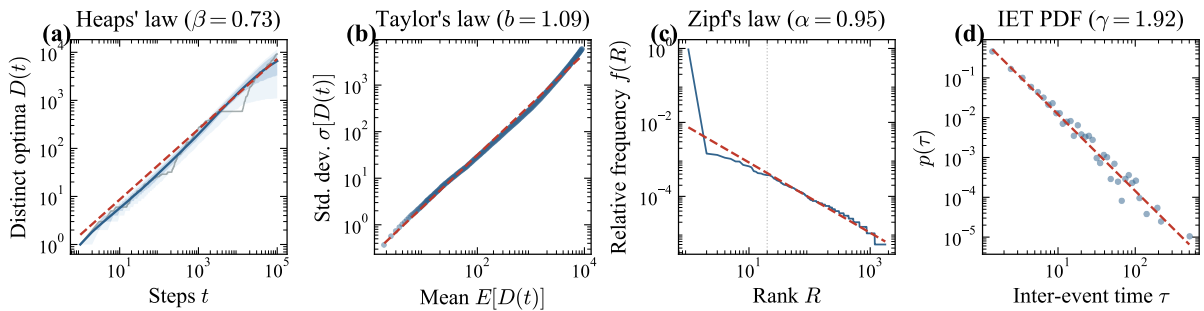


Figure 8: Ensemble results with higher persistence ( $\rho = 0.9$ ,  $\varepsilon = 0$ ; all other parameters as in Figure 6). Fitted exponents:  $\beta = 0.732$ ,  $b = 1.091$ ,  $\alpha = 0.950$ ,  $\gamma_{\text{IET}} = 1.922$ .

The effects are in several respects the opposite of the fewer-octaves case. The Heaps exponent decreases modestly to  $\beta = 0.732$ , but here the slowdown arises not from fewer optima but from denser local cycling among many small basins without substantial progress toward unexplored communities. The Zipf exponent drops below unity to  $\alpha = 0.950$ , reflecting the proliferation of small basins that dilutes the dominance of top-ranked attractors. The Taylor exponent rises to  $b = 1.091$  because the larger number of heterogeneous communities makes each walker's early trajectory more consequential. The inter-event time exponent increases to  $\gamma_{\text{IET}} = 1.922$ , indicating a slightly lighter tail: denser local structure provides more inter-basin transitions within each community, shortening typical waiting times even as the overall discovery rate is slower.

The contrast between the two variations is instructive. Both slow novelty growth, but through opposite structural mechanisms: removing fine-scale detail creates deeper traps, while adding it creates denser local cycling. Their signatures in the remaining exponents diverge accordingly: fewer octaves concentrates visits ( $\alpha$  up) and produces heavier inter-event tails ( $\gamma_{\text{IET}}$  down), while higher persistence disperses visits ( $\alpha$  down) and produces lighter tails ( $\gamma_{\text{IET}}$  up). This confirms that the four exponents are jointly constrained by LON structure and that different routes to slower novelty growth leave distinct fingerprints in the other three regularities.

### 5.7.3 Introducing exogenous innovation

Figure 9 shows the ensemble results when a small exogenous innovation rate  $\varepsilon = 10^{-5}$  is introduced, with all other parameters at baseline. At each step the walker now has a probability  $\varepsilon$  of teleporting to a uniformly random node, regardless of the current position or local edge structure.

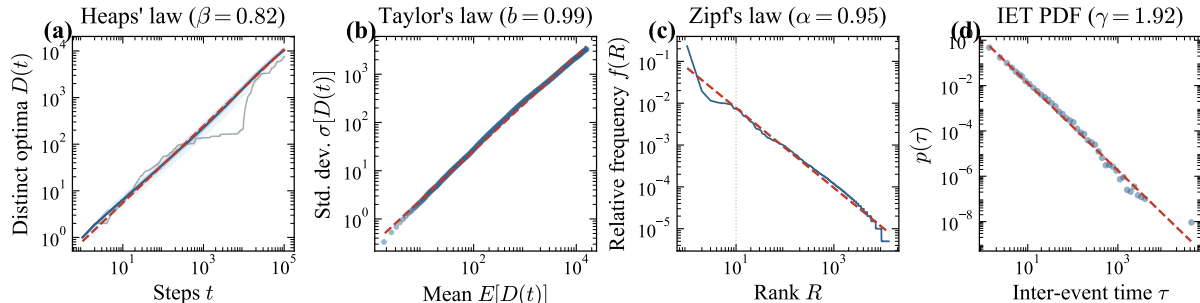


Figure 9: Ensemble results with exogenous innovation ( $\varepsilon = 10^{-5}$ ,  $n = 7$  octaves; all other parameters as in Figure 6). Fitted exponents:  $\beta = 0.777$ ,  $b = 0.990$ ,  $\alpha = 1.066$ ,  $\gamma_{\text{IET}} = 1.867$ .

The effects are modest but interpretable. Novelty growth is marginally faster ( $\beta = 0.777$ ) because occasional random jumps bypass inter-community bottlenecks. Visit concentration decreases ( $\alpha = 1.066$ ) as teleportation redistributes mass more evenly. Cross-replication variability decreases slightly ( $b = 0.990$ ) because all walkers eventually sample a broad cross-section of the LON. The inter-event time exponent increases marginally ( $\gamma_{\text{IET}} = 1.867$ ) as teleportation truncates the longest quiescent intervals. At  $\varepsilon = 10^{-5}$  and  $T = 200,000$  steps the expected number of teleportation events per walk is only two, yet this is sufficient to prevent the most extreme forms of lock-in. Exogenous innovation thus acts as a weak regularizer: it smooths the most extreme consequences of trapping without altering the qualitative character of the innovation record.

## 6 Discussion

The LON-innovation model developed in this paper demonstrates that a single structural object, the Local Optima Network, can generate the four main empirical regularities of the discovery-process tradition while retaining the basin-level, performance-ordered representation characteristic of the adaptive-search tradition. The parameter variations of Section 5.7 show, moreover, that the four exponents respond to changes in landscape ruggedness ( $\rho$ ), landscape complexity ( $n$ ), and exogenous innovation ( $\varepsilon$ ) in interpretable, jointly constrained ways. This section discusses the scope conditions of the current framework, its limitations, and the most promising directions for extension.

### 6.1 Scope and Limitations of the Baseline Model

The baseline model makes several simplifying choices that should be made explicit. The landscape is two-dimensional, which preserves all qualitative features of interest (multiple optima, basins, communities, ruggedness variation) but limits the combinatorial richness of the configuration space relative to the high-dimensional binary strings of NK models.

The walker dynamics are Markovian: the transition probability at each step depends only on the current node, not on the history of the walk. This rules out reinforcement effects, memory, and learning within the current formulation. The baseline operates with  $\varepsilon = 0$ , and even when exogenous innovation is introduced, the  $\varepsilon$ -teleportation mechanism imposes a structureless form of it: jumps are uniformly random and independent of the walker’s current fitness, the fitness of potential targets, or the behavior of other agents. Each of these simplifications points toward a natural extension.

## 6.2 Alternative Walker Dynamics

The baseline model deliberately adopts the simplest possible dynamics: a memoryless random walker whose transition probabilities are given directly by the basin-hopping weights  $w_{ij}$ . This isolates the contribution of LON topology to the observed regularities without introducing additional behavioral parameters.

Several richer dynamics are worth exploring. A *temperature-modulated walker* would bias transitions toward higher-fitness neighbors, with a temperature parameter interpolating between the baseline uniform dynamics and greedy climbing on the LON. This would be relevant for settings in which innovating agents preferentially pursue improvements, potentially producing tighter visit concentration and longer trapping episodes. An *edge-reinforced random walk* (Iacopini et al., 2018) would update transition probabilities as a function of past traversals, generating endogenous preferential reuse and a form of learning or habit formation. The results of Section 5 show, however, that the baseline walker already generates all four regularities within empirically observed ranges, validating the choice of starting with a minimal behavioral model.

## 6.3 From Isolated Walkers to Interacting Agents

The baseline model considers a single walker in isolation. In real innovation systems, firms, inventors, and research teams observe one another, imitate successful strategies, and compete for the same performance peaks. A natural extension is an agent-based model (ABM) in which multiple walkers navigate the same LON simultaneously, with the  $\varepsilon$ -teleportation mechanism replaced by a fitness-directed imitation rule: an agent observes the current positions and fitness levels of other agents and, with some probability proportional to the fitness differential, jumps toward a better-performing peer. This endogenizes the direction of long-range jumps, introduces a social dimension to exploration, and generates a natural coupling between the discovery processes of different agents.

The ABM extension also opens the door to studying the distinction between local and system-level novelty. With multiple walkers, a configuration can be new to one agent but already known to others, and the rate at which system-level novelty grows will depend on the degree of overlap in exploration trajectories. Imitation tends to increase this overlap, creating a trade-off between individual efficiency and collective diversity of exploration that is central to the organizational search literature (March, 1991; Baumann et al., 2019).

## 6.4 Multi-Landscape Dynamics and Radical Innovation

The baseline model operates on a single landscape, with communities serving as the operational definition of distinct technological paradigms. However, the history of technology

also features episodes of radical discontinuity in which an entirely new performance landscape emerges, rendering the old one obsolete: the transition from vacuum tubes to semiconductors, from film to digital photography, or from internal combustion to electric propulsion. A natural extension is a multi-landscape model in which the walker (or population of walkers) can transition from the current landscape  $\mathcal{L}^{(k)}$  to a newly generated landscape  $\mathcal{L}^{(k+1)}$  with a potentially higher performance ceiling. The re-initialization of agents at low-fitness positions in the new landscape would capture the Schumpeterian logic of creative destruction (Schumpeter, 1939; Dosi, 1982). A sequence of landscapes with progressively higher ceilings would also allow the model to generate long-run performance growth (Nelson and Winter, 1982), connecting the short-run regularities studied here to the long-run trajectories studied in the technological change literature.

## 6.5 Empirical Strategies

The model generates several testable predictions that could, in principle, be confronted with data. The most direct empirical strategy is to estimate the four exponents ( $\beta$ ,  $\alpha$ ,  $b$ ,  $\gamma_{\text{IET}}$ ) from patent, publication, or product-innovation data and compare them to the exponent ranges produced by the model under different parameterizations. The parameter variations of Table 2 show that the model generates a non-trivial joint structure among the four exponents: for instance, smoother landscapes (fewer octaves) slow novelty growth while concentrating visits and producing heavier inter-event tails, whereas more rugged landscapes (higher persistence) also slow novelty growth but disperse visits and produce lighter tails. These distinct joint signatures provide sharper tests than would be available from any single exponent alone. A more structural approach would attempt to reconstruct the LON, or at least its community structure and degree distribution, from observed sequences of technological choices. Citation networks among patents (Price, 1965), recombination networks among components (Fleming and Sorenson, 2001), and co-occurrence networks among technological codes (Aharonson and Schilling, 2016) all provide empirical network representations of technological relatedness and knowledge flow that may serve as partial proxies for the basin-transition structure that the LON formalizes.

## 6.6 Alternative Landscape Generation Mechanisms

The LON framework is not tied to the fBm landscape generator used here. A natural alternative is the NK model (Kauffman, 1993; Levinthal, 1997), the standard benchmark in the organizational search literature, which offers tunable ruggedness through the epistasis parameter  $K$  and fine-grained control over interdependence structure (Frenken, 2006a; Ethiraj and Levinthal, 2004). The LON construction procedure of Section 3.3 applies without modification to NK landscapes, and the resulting NK-LONs have been extensively characterized in the optimization literature (Ochoa et al., 2008; Vérel et al., 2011; Ochoa et al., 2014). Comparing innovation-record statistics from fBm-LONs versus NK-LONs would establish the robustness of the regularities documented in Section 5 to the choice of generator. Beyond NK, other generators of interest include block models with modular interaction structures, random field models with long-range correlations, and empirically calibrated landscapes constructed from patent or product data.

## 6.7 Higher-Dimensional Landscapes and Computational Scalability

The two-dimensional configuration space used throughout this paper enables tractable exhaustive enumeration of all local optima and their basins, but real technological design spaces are vastly higher-dimensional. Extending the model to  $d > 2$  dimensions is conceptually straightforward, since the Clifford torus mapping and fBm construction generalize naturally, but computationally demanding: exhaustive hill climbing from every grid point scales as  $L^d$ , making full enumeration infeasible for large  $d$ . Sampling-based LON construction methods, including the Markov-chain and snowball samplers discussed in Section 2.3, offer a path forward, but the relationship between sampled and exhaustive LONs in high dimensions requires further study.

## 7 Conclusion

This paper has introduced a model of innovation dynamics grounded in Local Optima Networks. The model constructs a LON from a toroidal fitness landscape generated via four-dimensional Perlin noise, identifies communities in the LON as technological paradigms, and studies stochastic walkers on the resulting network as a representation of innovating agents.

The central result is that walks on LONs simultaneously generate the four main empirical regularities of the discovery-process tradition: sublinear novelty growth (Heaps' law), heavy-tailed rank-frequency distributions (Zipf's law), anomalous fluctuation scaling (Taylor's law), and power-law distributed inter-event times, with fitted exponents that fall within the ranges commonly reported in empirical innovation data. All four emerge from the same structural features of the LON: the heterogeneous distribution of self-loop weights, the community organization of basins into distinct technological paradigms, and the fitness-degree correlations that concentrate visits on a small number of high-performance attractors. The model thereby provides a bridge between the discovery-process and adaptive-search traditions, connecting the sequence-level statistical regularities emphasized by the former to the basin-level, performance-ordered landscape structure emphasized by the latter.

Parameter variations show that the exponents are jointly constrained by the LON's structural properties and respond to changes in interpretable, structurally grounded ways. Different routes to the same macroscopic outcome leave distinct signatures in the remaining exponents, making the model's predictions falsifiable at the level of exponent vectors, not just individual scaling laws.

The framework is parsimonious: the landscape is controlled by a small number of parameters, the LON construction is governed by the perturbation radius, and the walker dynamics require only an optional exogenous innovation rate, which can be set to zero without losing any of the four regularities. Yet despite this parsimony, the model admits natural extensions to multi-agent settings with fitness-directed imitation, to multi-landscape settings with radical technological transitions, to alternative walker dynamics such as temperature-biased or edge-reinforced walks, and to alternative landscape generators including NK models.

The LON representation does not replace either the discovery-process or the adaptive-

search tradition. It provides a common formal object through which their distinct explanatory targets can be connected, and it makes the structural assumptions underlying innovation dynamics explicit, interpretable, and amenable to empirical testing.

## References

- Aharonson, B. S. and Schilling, M. A. (2016). Mapping the technological landscape: Measuring technology distance, technological footprints, and technology evolution. *Research Policy*, 45(1):81–96.
- Aletti, G. and Crimaldi, I. (2021). Twitter as an innovation process with damping effect. *Scientific Reports*, 11:21243.
- Aletti, G., Crimaldi, I., and Ghiglietti, A. (2023). Interacting innovation processes. *Scientific Reports*, 13(1):17187.
- Aletti, G., Crimaldi, I., and Ghiglietti, A. (2025). Central limit theorems for interacting innovation processes, related statistical tools and general results. *arXiv preprint arXiv:2501.09648*.
- Barabási, A.-L. (2005). The origin of bursts and heavy tails in human dynamics. *Nature*, 435:207–211.
- Baumann, O., Schmidt, J., and Stieglitz, N. (2019). Effective search in rugged performance landscapes: A review and outlook. *Journal of Management*, 45(1):285–318.
- Bellina, A., De Marzo, G., and Loreto, V. (2025). Full spectrum of novelties in time-dependent urn models. *Physical Review Research*, 7(2):023127.
- Billinger, S., Stieglitz, N., and Schumacher, T. R. (2014). Search on rugged landscapes: An experimental study. *Organization Science*, 25(1):93–108.
- Blackwell, D. and MacQueen, J. B. (1973). Ferguson distributions via Pólya urn schemes. *The Annals of Statistics*, 1(2):353–355.
- Chicano, F., Daolio, F., Ochoa, G., Verel, S., Tomassini, M., and Alba, E. (2012). Local optima networks, landscape autocorrelation and heuristic search performance. In *Parallel Problem Solving from Nature – PPSN XII*, volume 7492 of *Lecture Notes in Computer Science*, pages 337–347. Springer.
- Cleghorn, C. W. and Ochoa, G. (2021). Understanding parameter spaces using local optima networks: A case study on particle swarm optimization. In *Proceedings of the 2021 Genetic and Evolutionary Computation Conference Companion*, pages 1657–1664. ACM.
- De Marzo, G., Pandolfelli, F., and Servedio, V. D. (2022). Modeling innovation in the cryptocurrency ecosystem. *Scientific Reports*, 12(1):12942.
- Dosi, G. (1982). Technological paradigms and technological trajectories: A suggested interpretation of the determinants and directions of technical change. *Research Policy*, 11(3):147–162.
- Ethiraj, S. K. and Levinthal, D. (2004). Modularity and innovation in complex systems. *Management Science*, 50:159–173.

- Fleming, L. and Sorenson, O. (2001). Technology as a complex adaptive system: Evidence from patent data. *Research Policy*, 30(7):1019–1039.
- Frenken, K. (2006a). A fitness landscape approach to technological complexity, modularity, and vertical disintegration. *Structural Change and Economic Dynamics*, 17(3):288–305.
- Frenken, K. (2006b). Technological innovation and complexity theory. *Economics of Innovation and New Technology*, 15(2):137–155.
- Ganco, M., Kapoor, R., and Lee, G. K. (2020). From rugged landscapes to rugged ecosystems: Structure of interdependencies and firms’ innovative search. *Academy of Management Review*, 45(3):646–674.
- Homolya, V. and Vinkó, T. (2019). Memetic differential evolution using network centrality measures. *AIP Conference Proceedings*, 2070(1):020023.
- Homolya, V. and Vinkó, T. (2020). Leveraging local optima network properties for memetic differential evolution. In Le Thi, H. A., Le, H. M., and Pham Dinh, T., editors, *Optimization of Complex Systems: Theory, Models, Algorithms and Applications*, volume 991 of *Advances in Intelligent Systems and Computing*, pages 109–118. Springer, Cham.
- Iacopini, I., Di Bona, G., Ubaldi, E., Loreto, V., and Latora, V. (2020). Interacting discovery processes on complex networks. *Physical Review Letters*, 125:248301.
- Iacopini, I., Milojević, S., and Latora, V. (2018). Network dynamics of innovation processes. *Physical Review Letters*, 120:048301.
- Kauffman, S. A. (1993). *The Origins of Order: Self-Organization and Selection in Evolution*. Oxford University Press.
- Khraisha, T. (2020). Complex economic problems and fitness landscapes: Assessment and methodological perspectives. *Structural Change and Economic Dynamics*, 52:390–407.
- Levinthal, D. A. (1997). Adaptation on rugged landscapes. *Management Science*, 43(7):934–950.
- Li, F., Chen, J., and Ying, Y. (2019). Innovation search scope, technological complexity, and environmental turbulence: A nk simulation. *Sustainability*, 11(16):4279.
- March, J. G. (1991). Exploration and exploitation in organizational learning. *Organization Science*, 2(1):71–87.
- Mostert, W., Malan, K. M., Ochoa, G., and Engelbrecht, A. P. (2019). Insights into the feature selection problem using local optima networks. In Liefvooghe, A. and Paquete, L., editors, *Evolutionary Computation in Combinatorial Optimization*, volume 11452 of *Lecture Notes in Computer Science*, pages 147–162. Springer, Cham.
- Nelson, R. R. and Winter, S. G. (1982). *An Evolutionary Theory of Economic Change*. Harvard University Press.
- Ochoa, G., Tomassini, M., Vérel, S., and Darabos, C. (2008). A study of NK landscapes’ basins and local optima networks. In *Proceedings of the 10th Annual Conference on Genetic and Evolutionary Computation (GECCO)*, pages 555–562.

- Ochoa, G., Verel, S., Daolio, F., and Tomassini, M. (2014). Local optima networks: A new model of combinatorial fitness landscapes.
- Perlin, K. (1985). An image synthesizer. *ACM SIGGRAPH Computer Graphics*, 19(3):287–296.
- Pitman, J. and Yor, M. (1997). The two-parameter Poisson–Dirichlet distribution derived from a stable subordinator. *The Annals of Probability*, 25(2):855–900.
- Pons, P. and Latapy, M. (2006). Computing communities in large networks using random walks. *Journal of Graph Algorithms and Applications*, 10(2):191–218.
- Price, D. J. d. S. (1965). Networks of scientific papers. *Science*, 149(3683):510–515.
- Schumpeter, J. A. (1939). *Business Cycles*, volume 1. McGraw-Hill.
- Teixeira, M. C. and Pappa, G. L. (2022). Understanding AutoML search spaces with local optima networks. In *Proceedings of the Genetic and Evolutionary Computation Conference*, pages 449–457. ACM.
- Thomson, S. L., Le Goff, L., Hart, E., and Buchanan, E. (2024). Understanding fitness landscapes in morpho-evolution via local optima networks. In *Proceedings of the Genetic and Evolutionary Computation Conference*, pages 114–123. ACM.
- Thomson, S. L., Ochoa, G., Verel, S., and Veerapen, N. (2020). Inferring future landscapes: Sampling the local optima level. *Evolutionary Computation*, 28(4):621–641.
- Tria, F., Crimaldi, I., Aletti, G., and Servedio, V. D. P. (2020). Taylor’s law in innovation processes. *Entropy*, 22(5):573.
- Tria, F., Loreto, V., and Servedio, V. D. P. (2018). Zipf’s, heaps’ and taylor’s laws are determined by the expansion into the adjacent possible. *Entropy*, 20(10):752.
- Tria, F., Loreto, V., Servedio, V. D. P., and Strogatz, S. H. (2014). The dynamics of correlated novelties. *Scientific Reports*, 4:5890.
- Vérel, S., Ochoa, G., and Tomassini, M. (2011). Local optima networks of NK landscapes with neutrality. *IEEE Transactions on Evolutionary Computation*, 15(6):783–797.
- Wright, S. (1932). The roles of mutation, inbreeding, crossbreeding, and selection in evolution. In *Proceedings of the Sixth International Congress of Genetics*, volume 1, pages 356–366.